ISSN 1063-7729, Astronomy Reports, 2007, Vol. 51, No. 2, pp. 100–108. © Pleiades Publishing, Ltd., 2007.
Original Russian Text © A.A. Kisselev, Yu.N. Gnedin, E.A. Grosheva, N.A. Shaht, D.L. Gorshanov, M.Yu. Piotrovich, 2007, published in Astronomicheskiĭ Zhurnal, 2007, Vol. 84, No. 2, pp. 118–127.

The Supermassive Black Hole at the Center of Our Galaxy: Determination of Its Main Physical Parameters

A. A. Kisselev, Yu. N. Gnedin, E. A. Grosheva, N. A. Shaht, D. L. Gorshanov, and M. Yu. Piotrovich

Main Astronomical Observatory, Pulkovo, St. Petersburg, Russia

Received May 24, 2006; in final form, July 7, 2006

Abstract—We have used two astrometric methods developed at the Main Astronomical Observatory of the Russian Academy of Sciences—the method of apparent-motion parameters (AMP) and a direct geometrical method (DGM)—to derive the orbit of the star S2 around the Galactic center, and thereby the mass of the supermassive black hole at the Galactic center. The AMP method, which is based on measurements of the curvature of a fairly short orbital arc, is efficient if observational data on the relative radial velocity are available. The mass of the supermassive black hole was also estimated using astrophysical methods, based on the empirical relation between the masses of the supermassive black holes at the centers of galaxies and quasars and the radio and X-ray luminosities of these regions. We estimate the magnetic-field strength near the event horizon of the supermassive black hole at the Galactic center using a synchrotron self-absorption model.

PACS numbers : 98.35.Jk, 98.38.Am
DOI: 10.1134/S1063772907020047

1. INTRODUCTION

There is no longer any doubt that the centers of all galaxies host supermassive black holes. The most reliable basis for this statement is the discovery of strong X-ray emission from the central regions of galaxies with physical characteristics (such as the variability timescale) that agree well with the model of accretion onto a supermassive black hole (SMBH). However, the decisive role in identifying the nature of the central massive object in our Galaxy has been played by observations of stellar motions in the closest vicinity of the Galactic center [1–9]. These observations have enabled the detection of real stellar motions in the central parsec of the Galaxy, 8 kpc from the Sun, and the derivation of the orbits of these stars.

Additional important information on the physical parameters of the central SMBH can be derived from the radio and X-ray emission in its closest vicinity. Key information can be derived by analyzing the variability of this radiation. Simultaneous observations in various energy bands can reveal the physical mechanism that is responsible for the radiation of the plasma in the immediate vicinity of the SMBH.

A simultaneous burst of emission in X-rays and the infrared was first discovered by Eckart et al. [10]. The X-ray luminosity during the outburst was 6×10^{33} erg/s.

Strong variability of the source Sgr A* in the radio was also discovered, on timescales from hours to several years [11-13]. The short variability timescale imposes strong constraints on the scale of the radio-emitting region of ~ 10 AU, fairly close to the gravitational radius of a SMBH.

Studies of stellar dynamics in the vicinity of the SMBH at the Galactic center provide unique possibilities for testing post-Newtonian gravitational theory. Recently, Zucker et al. [14] showed that infrared stellar spectroscopy could be used for precise measurements of Doppler shifts in radial-velocity curves, which, in principle, can be used to derive corrections to the classical Newtonian theory—the gravitational redshift due to the SMBH, as well as the transverse Doppler shift of the spectral lines ($\sim v^2/c^2$).

However, the most interesting problem may be determining the physical nature and distribution of matter at the dynamical center of the Galaxy, whose total mass can be derived from observational data on the orbital motions of nearby stars. It is expected that, in addition to the central SMBH, the Galactic center (central parsec) contains at least three more components: dense star clusters, gas, which itself has three components (neutral, ionized, and high-temperature), and dark matter of an unknown nature that has been captured by the gravitational field of the SMBH and accumulates in this field, as in a potential well [15–17].

Recently, several ground-based and orbiting telescopes detected a large excess flux of high-energy γ-ray energy from the Galactic center, including a flux of photons with energies close to 511 keV [18–20]. This can be well understood in a model in which dark matter consists of weakly interacting massive particles (WIMPs) that decay and annihilate each other. A most impressive recent result is the detection of an excess flux of γ-rays with energies of several TeV by HESS [17] during two observing sessions lasting ~ 4.7 and ~ 11.8 hr; the fluxes themselves were detected at the 6σ and 9σ levels, respectively. The emission came from a region $\sim 3'$ in size around the dynamical center of the Galaxy, Sgr A*.

A detailed analysis of the behavior of stars in the immediate vicinity of Sgr A* led Genzel et al. [2] to the following conclusions.

1. The surface density and brightness of stars in the immediate vicinity of the compact radio source Sgr A* (~ 10 light min) decrease with distance from the source, while the volume density of stars depends on the distance as R^{-2}. Inside the region with projected radius $<100''$, the surface brightness increases inward to a radius of $\sim 1''$, while the estimated density of stars ($K \leq 15^m$) has a weak dependence on the radius, possibly providing evidence for the presence of dark matter that is concentrated around the SMBH. The estimated size of this region is 0.34 ± 0.20 pc [22]. Curiously, the maximum of the surface brightness and density of stars with $K \leq 13^m$ occurs not at the Galactic center, but in the cluster IRS 16, located $\sim 2''$ to the east of Sgr A*.

2. There are several stellar populations in the central parsec: a cluster of red giants with typical lifetimes $\sim (1–10) \times 10^9$ yr, a cluster of old, bright blue supergiants with ages of $\sim (2–7) \times 10^6$ yr, and a cluster of bright ($K \approx 10^m–12^m$) intermediate-mass, asymptotic-branch giants with ages of $\geq 10^8$ yr.

3. Studies of the radial-velocity dispersions for the stars at distances of $1''–20''$ showed that this velocity dispersion depends on the radius as $\langle \Delta V \rangle^2 \sim R^{-1}$. Statistical modeling of these data enabled estimation of the gravitational mass concentrated within a region with a size much less than 10 light days: $(2–3.3) \times 10^6\ M_\odot$. In the meantime, Schödel et al. [23] estimated the central gravitating mass to be $(3.5 \pm 0.5) \times 10^6\ M_\odot$, based on an analysis of the orbits of 17 stars located within several light hours of Sgr A*. This provided an estimate for the density of matter apart from the mass of the SMBH: $\geq 2 \times 10^{17}\ M_\odot/\mathrm{pc}^3$. The upper limit for the proper motion of Sgr A* obtained by Reid et al. [24] of ≤ 20 km/s raised the upper limit for the density of this additional gravitational mass to $10^{19.5}\ M_\odot/\mathrm{pc}^3$. Moreover, Alexander et al. [25] were able to derive the density distribution for this matter:

$$\rho(R) = 1.2 \times 10^6 \left(\frac{R}{10''}\right)^{-\alpha} M_\odot/\mathrm{pc}^3, \qquad (1.1)$$

where $\alpha = 2.0 \pm 0.1$ for $R > 10''$ and $\alpha = 1.4 \pm 0.1$ for $R < 10''$. In the very central region around Sgr A*, the distribution of the density of the gravitational mass is [2]:

$$\rho(R) = \begin{cases} 3 \times 10^7\ M_\odot/\mathrm{pc}^3 \ \text{ for } \ R = 1'', \\ 7 \times 10^8\ M_\odot/\mathrm{pc}^3 \ \text{ for } \ R = 0.1''. \end{cases} \qquad (1.2)$$

The total mass in the vicinity of the SMBH is estimated to be $1.3 \times 10^4\ M_\odot$ for $R \leq 1''.6$.

The aim of the present paper is to determine the main physical properties of the dynamical center of the Galaxy, including the mass of the SMBH, specific angular momentum, and magnetic field outside the event horizon, using the results of astrometric and astrophysical observations of the central region of the Galaxy in a broad range of wavelengths.

The central part of our study describes the possibility of applying original methods for determining the orbits of binary stars developed at the Pulkovo Observatory to analyses of stellar dynamics near the Galactic center. These are two methods proposed by A.A. Kisselev:

1) a direct geometrical method (DGM) [26, 27],

2) a method based on apparent-motion parameters (AMP).

The latter method was initially developed by a group of researchers at the Main Astronomical Observatory of the Russian Academy of Sciences for studies of the orbits of artificial satellites, but later found wide application to the orbits of binary stars [28–33]. The modern AMP method (as applied to binaries) is based on the use of a high-precision, fairly dense series of the relative positions, trigonometric parallaxes, and relative radial-velocities of the binary components for an epoch close to the mean epoch for the astrometric observations. This enables the calculation of orbital elements and estimation of the total mass of the components using data for a short arc. For the well known star S2 this means that, instead of having to observe its orbit over 15 yr, it is enough to observe it for ~ 3 yr, if the series of observations is dense enough.

As a result, when the orbit is computed using the AMP method, the total mass plays the role of a pivotal parameter on which the residuals $O - C$, i.e., the best fit to the observed orbit, depend.

The DGM determines the orbit in a somewhat different way, and it is necessary to obtain the observed ellipse for the entire orbital period; the mass is

then derived directly from Kepler's third law using the known semi-major axis of the orbit and parallax.

Another aim of our study is to determine the magnetic field in the closest vicinity of the SMBH using methods developed in several astrophysical studies (see, e.g., [34–36]).

2. APPLICATION OF THE AMP METHOD TO DETERMINE THE ORBIT OF THE STAR S2 IN THE VICINITY OF Sgr A*

Starting from 1991, regular observations of objects in the star cluster at the Galactic center were carried out using an efficient IR camera (the MPE SHARP NIP Speckle Camera) of the NTT telescope of the European Southern Observatory. The resolution provided is sub-arcsecond. These observations yielded high-precision series of positions for more than ten stars orbiting Sgr A* (considered to coincide with the central SMBH). Combined with radial velocities obtained using one of the VLT telescopes of the European Southern Observatory, these data enabled determination of the orbits of these stars. A similar study was done using one of the telescopes of the Keck Observatory [3, 5, 9, 15, 23, 24, 37–39]. The stellar orbits derived from these two sets of observations are somewhat different; in two cases, the differences are substantial.

The orbit of S2 (or S0-2) has been derived most reliably, since it has the shortest period of revolution about the Galactic center—about 15 yr—and has already been observed for more than 10 yr. In this time, the star passed through three quarters of its apparent ellipse around Sgr A*—the compact radio source at the Galactic center believed to coincide with the SMBH. We applied the AMP method [28–33] to determine the orbit of S2 based on a short arc. The aim of our present study is to test how well it is possible to derive this orbit by applying the AMP method to an inhomogeneous series of observations, and to compare the results for this method with those for methods based on the complete orbital ellipse. We were interested in the question of whether four years of observations would be sufficient to determine the orbit.

In the AMP method, the orbit of a visual binary is determined from the position vectors and velocity of the companion, B, relative to the main component, A. In turn, the position vectors and velocities are calculated from an accurate series of relative positions, trigonometric parallaxes, and relative radial velocities derived for an epoch that is close to the mean epoch for the astrometric observations.

The orbit of S2 is interesting precisely because the series of observations is not dense and homogeneous. In addition, we did not have high-precision parallaxes and relative radial velocities. We will not discuss here the reliability and accuracy of the input data for our determination of the orbit using the AMP method.

2.1. Input Data

Distance. For the distance to S2, we used the estimated distance to the Galactic center obtained by Eisenhauer [9]: $R_0 = 7.62 \pm 0.32$ kpc.

Relative positions. The positions of S2 relative to the compact radio source Sgr A* were taken from Fig. 1 of [7], while the relative radial velocities were taken from Fig. 3 of that same paper. We adopted six positions at epochs 1994.32–1998.36 to determine the apparent motion parameters.

Total mass of the system. Our input estimate of this mass corresponds to the data of [7, 9]: 15 $M_\odot$ for S2 and $(4.1 \pm 0.6) \times 10^6 \left(\dfrac{R_0}{8\ \text{kpc}}\right)^3 M_\odot$ for the central body [4]; for the above distance, this gives $(3.5 \pm 0.5) \times 10^6\ M_\odot$. Further, in the process of refining the orbit, this estimate of the mass of Sgr A* was increased to $4 \times 10^6\ M_\odot$.

2.2. Computations

The key formula of the AMP method for the distance between the components requires the curvature of the trajectory:

$$r^3 = \pm k^2 \frac{\rho \rho_c}{\mu^2} \sin(\psi - \theta)\,(\text{AU})^3, \qquad (2.1)$$

where ρ is the distance between S2 and Sgr A* at the mean epoch of the chosen observed arc, θ the position angle at this epoch, μ the apparent motion of S2 relative to Sgr A*, ψ the position angle of the apparent motion, and ρ_c the radius of curvature of the observed arc,

$$k^2 = 4\pi^2 (M_\text{A} + M_\text{B})\,(\text{a.u})^3/\text{yr}^2]. \qquad (2.2)$$

The curvature of the trajectory ρ_c was calculated as follows. Two segments of the arc were chosen and tangents to them drawn at the points T_1 and T_2, corresponding to the mean epochs of the segments. The values of μ and the position angle ψ of the apparent motion of S2 relative to Sgr A* were calculated for these epochs:

$$\mu = \sqrt{\dot\rho^2 + \frac{\rho^2}{57.3^2}\dot\theta^2}\ \text{arcsec}, \qquad (2.3)$$

$$\psi = \theta \pm 90^\circ \mp \arcsin\frac{\dot\rho}{\mu}\ \text{deg} \qquad (2.4)$$

In the latter expression, in order to ensure the coincidence of the direction of tangent (ψ) and the direction of the growth of θ, the upper signs should be adopted if θ increases with time, and the lower signs if θ decreases with time. The time derivatives of ρ and θ and the positions at the mean epoch T_0, ρ_0 and θ_0, were calculated via a least-squares fit of the series of relative positions at the observed epochs (1994.32–1998.36). Further, the curvature was calculated using an approximation formula that corresponds to the definition of the radius of curvature in the differential geometry

$$\rho_c \approx \frac{T_2 - T_1}{|\psi_2 - \psi_1|}\bar{\mu}, \qquad (2.5)$$

where the angle ψ is in radians. Since the epoch $T = \dfrac{T_2 + T_1}{2}$ for which the curvature was calculated is close to, but not equal to, the median epoch of the observations T_0, the relative positions ρ_0 and θ_0 of S2 were first interpolated for the epoch T and only then used in the AMP method. As the result, the following input data were used for the AMP computations

Epoch T	1996.154
Angular distance ρ	$0.1578''$
Position angle θ	343.922°
Apparent motion μ	16.7 arcsec/yr
Position angle of the apparent motion ψ	218.2°
Trajectory curvature radius ρ_c	$0.065''$
Relative radial velocity V_r	180 km/s
Mass of the system M_{A+B}	$4 \times 10^6\ M_\odot + 15\ M_\odot$
Parallax $\pi_{\rm tr}$	0.13 milliarcsec.

In the AMP method, the orbit is computed for a given separation component separation r and space velocity V of component B relative to component A, which are derived from the parameters of the apparent motion, radial velocity, and parallax.

The semi-major axis a and orbital period P are determined, as in other methods, from the energy integral for the two-body problem and Kepler's third law.

The orbital motion is considered in a reference frame with its origin coincident with the main component. The X and Y axes are directed like tangential coordinates in photographic astrometry, while the Z axis is directed away from the observer.

Further, unit position and velocity vectors $\mathbf{R}$ and $\mathbf{V}$ are calculated. The position vector $\mathbf{R}$ depends on its orientation relative to the plane of the sky. The angle between the plane of the sky and the position vector of component B, β, is determined from the relation

$$\cos\beta = \frac{\rho}{r\pi_{\rm tr}}. \qquad (2.6)$$

The position vector calculated in this way has two values, corresponding to the two possible signs of β, and is located either in front of or behind the plane of the sky. As a result, we obtain two orbits with different geometries. Identifying the real orbit requires invoking additional observations that are shifted in time from the main short arc [31]. In the case considered here, the two possible values were $\beta = \pm 44°$, and $\beta = +44°$ was identified as the value that satisfies the observations.

After determining $\mathbf{R}$ and $\mathbf{V}$, we can find the orbital orientation parameters and epoch of periastron passage using classical methods based on Kepler's laws and the eccentricity. We should note that the orbital inclination is uniquely defined: $0° < i < 90°$ if $\cos i > 0$, i.e., if the direction of apparent motion of the companion in the orbit coincides with rotation from X to Y in the plane of the sky ($\dot\theta < 0$), and $90° < i < 180°$ if $\cos i < 0$, i.e., the apparent motion is in the opposite direction ($\dot\theta > 0$).

We thus obtain all the elements of the visual binary's orbit:

$$a, P, e, \omega, i, \Omega, \text{ and } T_{\rm P}.$$

Our results for these elements are listed in the second row of Table 1. The first row of Table 1 lists the results for the orbital elements derived from the apparent orbital ellipse with the direct geometrical method, which uses the precise geometrical relations between the parameters of the true ellipse and its projection onto the plane of the sky, including the projection of the star at the focus of the true ellipse [26, 27]. For comparison, we also list in Table 2 the orbital elements derived from the observed orbital ellipse earlier in other studies.

We will make two comments concerning Table 2.

1. When the inclinations were calculated in a different way, we give in parentheses the inclinations calculated in the astrocentric reference frame.

2. The derivation of different longitudes of the ascending node is due to the different choices of reference frame and direction of increasing angle. When the angles were measured differently than in the DGM, we give in parentheses the angle in the astrocentric reference frame, which increase in the direction of the orbital motion. (The difference in the

Table 1. Orbital periods of S2 calculated using the direct geometrical method (DGM) and the apparent ellipse and using the apparent motion parameters (AMPs)

Method	a	P	e	ω	i	Ω	T_P	$M_{A+B}, M_\odot$
DGM	849.2	15.9	0.832	233.2	43.7	35.0	2002.3	2.07×10^6
AMP	924.8277	14.06	0.820	235.3	55.4	26.24	2002.592	$4 \times 10^6 + 15$

Table 2. Orbital solutions for S2 obtained in various studies

Reference	a	P	e	ω	i	Ω	T_P	$M_A, 10^6 M_\odot$
Ghez et al. 2003 [4]	996.8254	15.78	0.8736	248.5	−47.3	49.9	2002.334	4.07
Eisenhauer et al. 2005 [8]	893.6508	15.24	0.866	62.6	131.9 (48.1)	221.9 (41.9)	2002.315	4.06
Ghez et al. 2005 [5]	919	14.53	0.867	242.8	135.2 (44.8)	44	2002.308	3.67
Schödel et al. 2003 [23]	944.4444	15	0.87	250	46	36	2002.3	3.70

longitudes of the ascending node is due to the two-valued nature of the transition from the apparent to the true orbital ellipse when the classical methods are applied. Applying the DGM, which uses the relative orbital velocity, makes it possible to obtain a unique solution to the problem.)

Figures 1 and 2 show how well the derived orbits fit the observations. Figure 2 shows that the DGM orbit derived from six observations in 1994.32–1998.36 is quite similar to the orbit derived using geometrical methods, but deviates close to periastron. We believe this inconsistency is a consequence of the use of insufficient input data: the series of observations used is not homogeneous, the number of points is small, and precise radial velocities were not known.

2.3. Conclusion

The DGM does not require long observations: a short arc and relative radial velocities are sufficient to derive the orbit. Though the mass of the system is not derived by the DGM, so that previously known values must be used, this method can serve as a means of indirect verification of the correctness of the masses used, via a comparison of the ephemerides and observations. In this case, the mass can serve as a parameter that may be varied in order to reduce the residuals, $O - C$.

Our comparison of the orbits of S2 determined with the DGM using an almost complete orbital ellipse and with the AMP method using a short arc indicates the following. If the DGM is applied to a series of observations that has similar precision and density as the series of observations for S2, this method is quite satisfactory for estimating the orbital elements, and can be applied to other stars orbiting the Galactic center for which only short arcs have been observed. This would be especially interesting for the two stars for which different groups have presented fundamentally different orbits (S0-1 and S04, see [37]; S1 and S8, see [9]). This requires a series of observations giving the stellar coordinates with precise epochs.

Moreover, there exists the possibility of refining the estimate of the gravitating mass by constructing a set of self-consistent (in terms of this mass) orbits for all stars close to the Galactic center that have been observed astrometrically.

3. ASTROPHYSICAL METHODS FOR DETERMINING THE MASS OF THE SMBH

There exist a number of astrophysical methods for determining the masses of SMBHs, which have been successfully applied to the active galactic nuclei (AGN) and quasars (see, e.g., [40]).

The most popular one establishes a direct relation between the mass of the SMBH in the active galactic nucleus and the dispersion σ of the stellar velocities and gas in its immediate vicinity (bulge)—so called "reverberation mapping." According to Gebhardt et al. [41], this relation is defined as :

$$M_{\rm BH} = 1.2 \times 10^8 M_\odot \left(\frac{\sigma}{200\ {\rm km/s}}\right)^{3.75}. \quad (3.1)$$

Taking $\sigma \approx 70$ km/s, in accordance with Gould and Quillen [42], we obtain $M_{\rm BH} = 2.4 \times 10^6 M_\odot$, in agreement with our DGM estimate and about a factor of 1.5 lower than our AMP estimate.

Another independent estimate can be derived from the empirical relations (fundamental-plane relations) found by Merloni et. al. [43–45] based on an analysis of observations of AGN and quasars over a broad

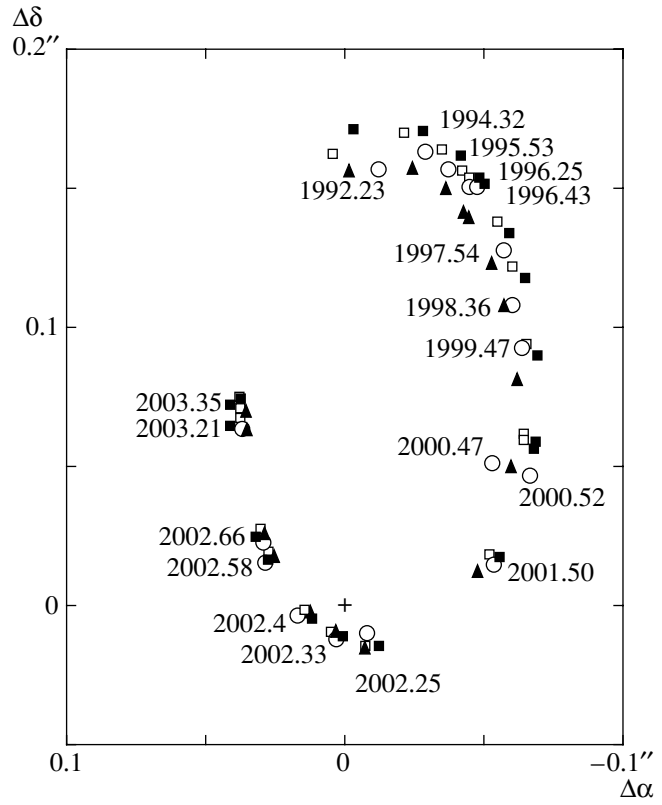

Fig. 1. Comparison of relative positions of S2 (circles) with the ephemerides obtained by Ghez et al. [4] (filled squares), Ghez et al. [5] (open squares), and Eisenhauer [8] (triangles).

range of wavelengths. It appears that all these objects are located in a "fundamental plane" in the three-dimensional physical parameter space formed by $\log L_{\rm R}$, $\log L_{\rm X}$, and $\log M$, where $L_{\rm R}$ and $L_{\rm X}$ are the radio and X-ray luminosities and M is the mass of the SMBH at the center of the galaxy or quasar in solar masses. The equation of the fundamental plane has the form [43]

$$\log L_{\rm R(5\ GHz)} = \left(0.60^{+0.11}_{-0.11}\right)\log L_{\rm X} + \left(0.78^{+0.11}_{-0.09}\right)\log M + 7.33^{+4.08}_{-4.07}. \quad (3.2)$$

Using the existence of a strong correlation between the radio and X-ray luminosities, Merloni et al. [43–45] were able to exclude the dependence on the X-ray luminosity from (3.2), and thereby to derive from (3.2) the simpler expression

$$\log L_{\rm R} = (28.75 \pm 0.18) + (1.20 \pm 0.04)\log M. \quad (3.3)$$

Curiously, radio and X-ray observations of Galactic stellar-mass black holes (microquasars [46]) were also used to derive (3.3).

Let us estimate the mass of the SMBH at the Galactic center using the observed spectral energy distribution (SED) for Sgr A* [47, 48] and relations (3.2) and (3.3).

At low frequencies, the maximum of the SED of Sgr A* is at $\nu_{\rm R} \approx 10^{12}$ Hz and the luminosity is $L_{\rm R} = 10^{36}$ erg/s. Equation (3.3) then gives the value $M_{\rm SMBH} \leq 2.5 \times 10^6 M_\odot$.

Using relation (3.2) with the radio luminosity at $\nu = 5$ GHz and the X-ray luminosity $L_{\rm X}$, we estimate the mass of Sgr A* to be $M_{\rm SMBH} = 4.16 \times 10^6 M_\odot$.

Of course, we should bear in mind that these estimates of the SMBH mass are only indicative, since they are subject to statistical scatter.

4. MAGNETIC FIELD NEAR THE EVENT HORIZON OF THE SMBH AT THE GALACTIC CENTER

It is commonly accepted that the energy and angular momentum of a rotating black hole is most efficiently transferred to the surrounding matter by processes associated with existence of an appreciable magnetic field in the vicinity of the black hole, which connects the black hole with the surrounding material

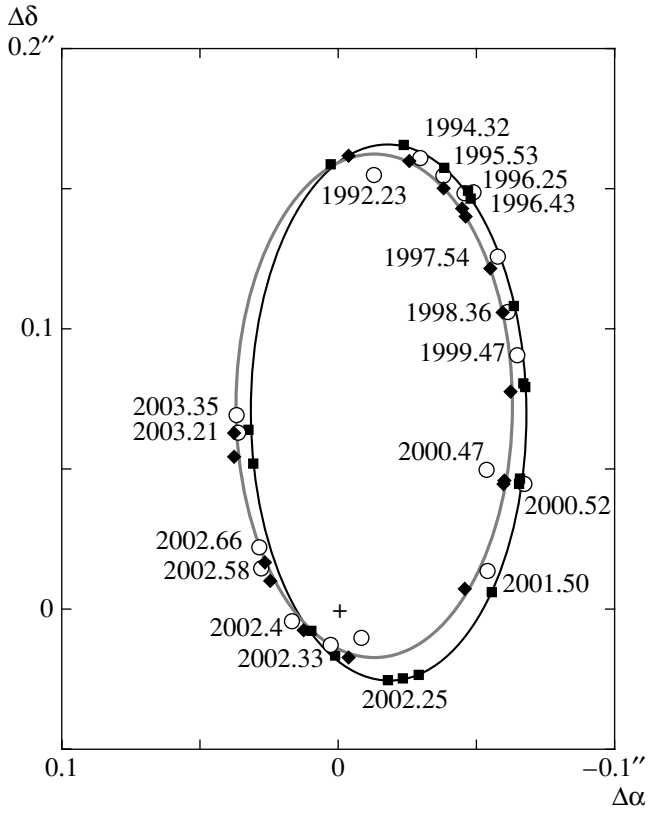

Fig. 2. Comparison of the orbit of S2 determined using the AMP method (squares) with the observational data (circles) and the orbit determined using the DGM and the observed ellipse (diamonds). The position of Sgr A* is marked by a cross.

(accretion disk). The theory of this process was developed in the classical paper by Blandford and Znajek [49].

Direct measurements of magnetic fields in AGN and quasars remains a major problem. Unfortunately, applying classical methods for magnetic-field measurements to these objects meets with substantial difficulties. There do exist several indirect methods (see the reviews [36, 50, 51]). One is based on the assumption that the densities of the magnetic and thermal energies in the gas immediately adjacent to the black hole are in equipartition. Using this assumption, Zhang et al. [52] derived the following correlation between the black-hole mass and the magnetic-field strength in the vicinity of the event horizon from the observational data:

$$\log B_{\rm BH} = 9.26 - 0.81 \log \left(M_{\rm BH}/M_\odot\right). \qquad (4.1)$$

The derivation of (4.1) made use of the well known relation between the luminosity of an AGN at $\lambda =$ 5100 Å and the mass of its SMBH.

Assuming that the mass of the central nucleus of the Galaxy is $3.5 \times 10^6 M_\odot$, we obtain, using (4.1), the magnetic-field strength

$$B_{\rm BH} = 2.5 \times 10^3 \text{ G}. \qquad (4.2)$$

If the assumed black-hole mass is $M_{\rm BH} = 2.5 \times 10^6 M_\odot$, the corresponding magnetic field is $B_{\rm BH} = 1.5 \times 10^4$ G.

Slysh [34] suggested another independent method for determining the magnetic field, based on synchrotron theory. According to [34], the magnetic field in the radio-emitting region of the compact object is

$$B = 10^{-5} b(\alpha) \left(\frac{\nu_p}{1\text{ GHz}}\right)^2 \theta^4 \left(\frac{1\text{ Jy}}{S_p}\right)^2, \qquad (4.3)$$

where ν_p is the frequency at which the optical depth for synchrotron self-absorption is unity, S_p is the flux density at that frequency, θ is the angular size of the radio source, $b(\alpha)$ is a numerical coefficient that depends on the spectral index of the synchrotron source in the optically thin region α, and we can assume $b(\alpha) \sim 1$ [53].

Assuming that the typical scale of the radio-emitting region is equal to the radius of the last stable orbit around the SMBH, we obtain using (4.3) the estimated magnetic-field strength $B(3R_g) \approx 300$ G; this corresponds to a field strength at the event horizon of $B_{\rm BH}(R_g) = 8.1 \times 10^3$ G, and is almost

identical to the estimates (4.1) and (4.2) obtained using an independent method.

5. ANGULAR MOMENTUM OF THE SUPERMASSIVE BLACK HOLE Sgr A*

Blandford and Znajek [49] suggested an interesting physical process that demonstrates how the energy of a rotating black hole can be extracted by means of the magnetic field generated in the accretion disk around black hole.

According to Blandford and Znajek [49], the maximum of energy that can be extracted is

$$L_{\rm BZ} = \left(\frac{B^2}{4\pi}\right)\pi R_{\rm H}^2\left(\frac{a}{R_{\rm H}}\right)^2 c, \qquad (5.1)$$

where $R_{\rm H} \approx GM/c^2$ is the radius of the event horizon of a rotating Kerr black hole and a is the specific angular momentum of the rotating black hole.

Using the luminosity of Sgr A* [46] and our estimate of the magnetic field, we can derive from (5.1) the ratio of the specific angular momentum of the rotation to the size of the event horizon (known in general relativity as the dimensionless ratio a/M in units in which $G = c = 1$).

If we assume that all the energy of the rotating black hole is transforms into radiation, $a/R_{\rm H} \approx 3 \times 10^{-3}$, providing evidence that Sgr A* is most likely a Schwarzschild black hole. Taking into account the fact that some fraction of the energy of rotation of the black hole is transformed into the kinetic energy of the matter flowing from the Galactic center, we suggest $a/R_{\rm H} \leq 0.01$.

6. MAIN RESULTS

Our main result here is our demonstration of the effectiveness of the AMP method, originally developed at the Main Astronomical Observatory of the Russian Academy of Science under the guidance of A.A. Kisselev and successfully applied to determine the parameters of visual binaries. Though this method, in principle, requires high-precision and fairly dense series of observations of the relative positions, as well as precise trigonometric parallaxes and relative radial velocities, it is also effective when not all these conditions are fully met. The advantage of the AMP method is that it does not require long observations of the total orbit, which, in the case of the Galactic center, require not less than 15 yr of observations. To apply the AMP method, it is sufficient to have a short arc of astrometric observations and the relative radial velocity for this arc.

There exist astrophysical methods for estimating the masses of SMBHs in Galactic nuclei. These methods are based on various empirical relations, such as the dependence between the mass of the black hole and the stellar and gas velocity dispersion in the bulge, and the relation between the radio and X-ray luminosities of the SMBH outside the event horizon and its mass. While these methods can be used to estimate the mass of the SMBH at the Galactic center, they are less precise than astrometric methods.

We have also estimated the magnetic field and specific angular momentum of the black hole. Our estimate of the angular momentum suggests that the SMBH at the Galactic center is a Schwarzschild rather than Kerr black hole, since we estimate the Kerr parameter to be $a/M \approx 0.01$ (in units with $G = c = 1$).

ACKNOWLEDGMENTS

This work was supported by three Basic Research Programs of the Russian Academy of Sciences: the program of the Presidium of the RAS "Origin and evolution of stars and galaxies", the program of the Physics Section of the RAS "Extended objects in the Universe", and a program of the St. Petersburg Scientific Center of the RAS. This study also was performed under contract with the Russian Ministry of Education and Science (Lot No. 14).

REFERENCES

1. R. Genzel, C. Pichon, A. Eckart, et al., Mon. Not. R. Astron. Soc. **317**, 348 (2000).
2. R. Genzel, R. Schodel, T. Ott, et al., Astrophys. J. **594**, 812 (2003).
3. A. M. Ghez, M. Morris, E. E. Becklin, et al., Nature **407**, 349 (2000).
4. A. M. Ghez, G. Duchêne, K. Matthews, et al., Astrophys. J. **586**, L127 (2003).
5. A. M. Ghez, S. Salim, S. D. Hornstein, et al., Astrophys. J. **620**, 744 (2005).
6. A. Eckart, R. Genzel, T. Ott, and R. Schödel, Mon. Not. R. Astron. Soc. **331**, 917 (2002).
7. F. Eisenhauer, R. Schödel, R. Genzel, et al., Astrophys. J. (Letters) **597**, L121 (2003).
8. F. Eisenhauer, R. Genzel, T. Alexander, et al., Astrophys. J. **628**, 246 (2005).
9. F. Eisenhauer, R. Genzel, T. Alexander, et al., astro-ph/0502128 (2005).
10. A. Eckart, F. K. Baganoff, M. Morris, et al., Astron. Astrophys. **427**, 1 (2004).
11. G. C. Bower, H. Falcke, R. J. Sault, and D. C. Backer, Astrophys. J. **571**, 843 (2002).
12. R. M. Herrnstein, J.-H. Zhao, G. C. Bower, and W. M. Goss, Astron. J. **127**, 3399 (2004).
13. J.-H. Zhao, K. H. Young, R. M. Herrnstein, et al., Astrophys. J. **586**, L29 (2003).

14. S. Zucker, T. Alexander, S. Gillessen, et al., astro-ph/0509105 (2005).
15. T. Ott, R. Schödel, R. Genzel, A. Eckart, et al., Messenger, No. 111, 1 (2003).
16. S. Nayakshin, J. Guadra, and R. Sunyaev, Astron. Astrophys. **413**, 173 (2004).
17. J. Hall and P. Gondolo, astro-ph/0602400 (2006).
18. W. Hofmann (For the HESS Collaboration), in *Proceedings of the 29th International Cosmic Ray Conference, Pune, India, 2005.*
19. P. Jean, J. Khödlseder, W. Gillard, et al., astro-ph/0509298 (2005).
20. A. Goldwurm, G. Belanger, P. Goldoni, et al., astro-ph/0407264 (2004).
21. S. S. Doeleman, et al., Astron. J. **121**, 2610 (2001).
22. R. Genzel, K. Thatte, A. Krabbe, et al., Astrophys. J. **472**, 153 (1996).
23. R. Schödel, T. Ott, R. Genzel, et al., Astrophys. J. **596**, 1015 (2003).
24. M. J. Reid, K. M. Menten, R. Genzel, et al., Astrophys. J. **587**, 208 (2003).
25. T. Alexander, Astrophys. J. **527**, 835 (1999).
26. A. A. Kisselev, in *Visual Double Stars: Formation, Dynamics and Evolutionary Tracks,* Astrophys. Space Sci. Library **223**, 357 (1997).
27. A. A. Kisselev, in *Astronomo-geodezicheskie issledovaniya. Blizkie dvoinye i kratnye zvezdy* (Astrogeodesical Investigations. Close Double and Multiple Stars) (UrGU, Sverdlovsk, 1990), p. 36 [in Russian].
28. A. A. Kisselev and O. P. Bykov, Astron. Zh. **53**, 879 (1975) [Sov. Astron. **20**, 496 (1975)].
29. A. A. Kisselev, O. P. Bykov, and L. I. Yagudin, Izv. Gl. Astron. Obs. Pulkovo, №. 198, 139 (1980).
30. A. A. Kisselev and O. V. Kiyaeva, Astron. Zh. **57**, 1227 (1980) [Sov. Astron. textbf24, 708 (1980)].
31. O. V. Kiyaeva, Astron. Zh. **60**, 1208 (1983) [Sov. Astron. **27**, 701 (1983)].
32. A. A. Kisselev, *Theoretical Fundamentals of Photographic Astrometry* (Nauka, Moscow, 1989) [in Russian].
33. A. A. Kisselev and L. G. Romanenko, Astron. Zh. **73**, 875 (1996) [Astron. Rep. **40**, 795 (1996)].
34. V.I. Slysh, Nature **199**, 682 (1963).
35. V. S. Artyuk and P. A. Chernikova, Astron. Zh. **78**, 20 (2001) [Astron. Rep. **45**, 16 (2001)].
36. Yu. N. Gnedin and M. Yu. Piotrovich, Astron. Lett. **32**, 431(2006).
37. A. M. Ghez, S.A. Wright, K. Mattews, et al., Astrophys. J. **601**, L159 (2004).
38. A. Eckart, R. Genzel, R. Hofmann, et al., Astrophys. J. **445**, L2 (1995).
39. A. Eckart, R. Genzel, T. Ott, R. Shoedal, Mon. Not. R. Astron. Soc. **331**, 917 (2002).
40. L. Ferrase, H. Ford, astro-ph/0411247 (2004).
41. Gebhardt *et al.*, Astrophys. J., **539**, L13 (2000).
42. A. Gould and A.C. Quillen, astro-ph/0302437 (2003).
43. A. Merloni, S. Heinz, and T. Di Matteo, astro-ph/0305261 (2003).
44. A. Merloni, S. Heinz, T. Di Maletto, Mon. Not. R. Astron. Soc. **345**, 1057 (2003).
45. A. Merloni, S. Heinz, T. Di Matteo, astro-ph/0410481 (2004).
46. A. M. Cherepashchuk, Usp. Fiz. Nauk **171**, 864 (2001) [Phys. Usp. **44**, 821 (2001)].
47. F. Ozel, D. Psaltis, and R. Narayan, Astrophys. J. **514**, 234 (2000).
48. F. Yuan, E. Quataert, and R. Narayan, astro-ph/0304125 (2003).
49. R. D. Blanford and R. L. Znaek, Mon. Not. R. Astron. Soc. **179**, 433 (1977).
50. Yu. N. Gnedin and T.M. Natsvlishvili, Astrophys. Space Phys. **10**, 1 (2000).
51. Yu. N. Gnedin and N. A. Silant'ev, Pis'ma Astron. Zh. **28**, 499 (2002) [Astron. Lett. **28**, 438 (2002)].
52. W.M. Zhang and Y. Lu, S.N. Zhang, astro-ph/0501365 (2005).
53. K. Hirotani, Astrophys. J. **619**, 73 (2005).

Translated by L. Yungel'son